LASERS

Junction lasers

Slices of semiconductor, formed into tiny, efficient, rugged and inexpensive lasers, combine sophisticated design with mass-market appeal.

L. A. D'Asaro and José E. Ripper

Junction lasers are devices in which laser action is produced by a high, nonequilibrium concentration of electrons and holes within the same small region of a semiconductor. Why do we want junction lasers? They are interesting not only from the viewpoint of the physics involved;[1] their properties suit them for industrial application as well. The advantages include:

- Smallness: Dimensions of the active region are typically one to two microns, with the largest dimension usually no more than a fraction of a millimeter.
- Mechanical stability: The mirrors are an integral part of the laser structure, and are usually formed by cleaving the crystal.
- High efficiency: Pulsed junction lasers have operated at as much as 40% external quantum efficiency.
- Reasonable power: Continuous output of 40 mW has been obtained at room temperature, with much higher powers at low temperatures. The record peak-power output in a 100-nanosec pulse is about 100 watts.
- Versatility: Junction lasers are conveniently pumped with direct current, and their output can be amplitude, frequency or pulse-position modulated into the GHz range. They can lase at wavelengths from 20 to 0.75 microns with the proper choice of semiconductor alloy, and can operate in a single mode. Within the last year, junction lasers have been operated continuously at room temperature.[2]

L. A. D'Asaro and José E. Ripper are both at Bell Telephone Laboratories, Murray Hill; D'Asaro is supervisor of the GaAs Laser Group and Ripper is a member of the group.

Any one of several methods that produce electron-hole pairs—optical or electron-beam excitation, avalanche multiplication in an electric field—can produce the desired nonequilibrium populations. Injecting electrons from the electron-rich (n) side to the hole-rich (p) side of the junction by applying a voltage in the direction of easy current flow is, however, the most practical method because of its efficiency and experimental simplicity, and here we shall concern ourselves only with such p–n junction lasers operating in forward bias.

Simple p–n junction lasers

An energy-band diagram of a p–n junction (see figure 2) shows the effect of forward bias. We see injection of electrons across the junction followed by recombination of electrons and holes, which corresponds to excitation and luminescence. The band structure of the semiconductor is critical. Lasing is likely only in a "direct-gap" structure, a structure in which electrons and holes have the same crystal momentum. In an "indirect-gap" semiconductor, a third particle (such as a phonon) must also be involved in the recombination to conserve crystal momentum. In this less favorable case the probability of stimulated emission is of the same order of magnitude as is the probability of transitions that lead to losses rather than to lasing.

To invert the carrier population, the product of the electron charge and the voltage across the junction must be greater than $h\nu$, where ν is the frequency of the emitted light. For this situation to exist, the Fermi level must be within either the valence or conduction bands on at least one side of the junction,[3] a situation known as "degenerate doping" of a semiconductor material (see figure 2).

Mode patterns from stripe-geometry double-heterostructure lasers. Diode 1 shows zero-order mode at 1.9 amps operating current; in 2, stripe width is increased, giving a first or second order mode along the junction; in 3, thickness is increased, producing third-order modes perpendicular to the junction. From ref. 29.
Figure 1

The laser cavity (see figure 3) is usually formed by two mirrors at the ends of the crystal. Semiconductors usually have a high refractive index, particularly for light of photon energy near the gap, so that a large enough discontinuity exists between the laser medium and air to form mirrors without any coating. Because crystals cleave along planes of

weakest binding, the mirrors will be parallel. Perpendicular to the junction, a small increase in the refractive index (0.01 for gallium arsenide) exists in the junction area, forming a dielectric waveguide that confines the radiation. In the other direction, along the junction but transverse to the emission, small random variations in the refractive index confine the radiation and form it into multiple filaments. Although several models have been proposed[4] to explain these variations, their origin remains unclear.

Studying the laser mode structure under these conditions is difficult, because the filaments are not constant in time and the mode spectra do not reproduce from run to run. This difficulty does not exist in the stripe-geometry laser (figure 4), where the active region is limited to a single filament.[5] In a structure with an appropriate stripe width, Hermite-Gaussian field distributions were observed, and high-resolution mode spectra were obtained.

One such spectrum, taken from a GaAs laser operating continuously at low temperature is shown in figure 5. The separation between two longitudinal modes of the same transverse distribution is inversely proportional to the length of the laser.

The narrowness of the observed width is limited by the spectrometer; interferometry has shown that for continuous-wave (cw) lasers the mode width can be less than 150 KHz (3×10^{-5} Å).[6]

In a junction laser the threshold current I_{th} (the minimum applied current at which lasing occurs) can often be fitted to an exponential function of the temperature T

$$I_{th} = I_0 e^{T/T_0}$$

where I_0 and T_0 are adjustable parameters. The spreading of the Fermi distribution of the minority carriers above the band edge partly explains the temperature dependence, because the population per energy interval then changes with temperature. But the temperature dependence of minority-carrier diffusion is also important; the diffusion coefficient decreases with decreasing temperature, resulting in an increase in population per unit volume at lower temperatures, if the current is held constant. Free-carrier absorption, a loss mechanism that decreases with decreasing temperature, is a factor as well.

These effects, all included in the equation above, resulted in ratios of threshold current of 50 or more between 77 K and 300 K for early GaAs lasers. Typical values of threshold-current density are 10^3 amps per cm^2 at 77 K and 5×10^4 amps per cm^2 at 300 K.

The thermal resistance between the junction and the heat sink together with the value and temperature dependence of the threshold current determine the maximum ambient temperature at which continuous lasing is possible. Simple lasers such as the one in figure 3 do not run continuously at room temperature, but are operated in pulses.

For lasing to occur, a spontaneously emitted photon must traverse the cavity with sufficient gain to avoid attenuation. Stated mathematically,

$$R \exp[(g-\alpha)L] = 1$$

or

$$g = \alpha + 1/L \log (1/R)$$

where g is the gain per unit length, α is the loss per unit length, L is the length of the cavity, and R is the reflectivity of the mirrors. The gain increases at least linearly with current density.

Heterostructure lasers

If we confine the carriers in the active region by a potential barrier, we reduce the temperature dependence of the threshold as well as its value. We can create such a barrier by putting a material with a higher energy gap near the junction. The choice of barrier material is important because states at the interface between different crystals will usually produce a high density of recombination centers, increasing the probability of nonlasing processes. On the other hand, certain crystal-lattice structures are excellently matched, and interfacial states between them are almost completely avoided. The most widely used of such materials are gallium arsenide and aluminum arsenide, which have lattice spacings that differ by only about 0.2% at most, and are exactly equal at 900 deg C. In the composition range for which the alloy is a direct-gap semiconductor, the band gap ranges from 1.4 up to 1.9 eV. A GaAs = $Al_xGa_{1-x}As$ interface shows negligibly few states compared with the GaAs surface-to-air interface.

The double-heterostructure laser diagrammed in figure 6 uses $Al_xGa_{1-x}As$ to combine low threshold current and high output efficiency. The active region of p-type GaAs is sandwiched between layers of n-type and p-type $Al_xGa_{1-x}As$, which have wider gap regions. Band-gap differences of a few kT (about 0.1 eV at 300 K) are sufficient to confine the carriers to the active region, and if $x = 0.08$ or more, we get the needed band-gap differences. The width d of the active region must be smaller than a minority-carrier diffusion length to achieve the desired lowering of the threshold. In high-quality GaAs at room temperature, the electron-diffusion length is several microns, so that useful values of d range from a few microns down; 0.3 microns is the smallest thickness now available. Because the threshold decreases proportionally with d, the smaller values are desirable.

The relative magnitudes of the potential barriers at the p–n heterojunction make it easier to inject electrons into the p-type active region (GaAs) than holes into the n-type region ($Al_xGa_{1-x}As$; see figure 6). The double heterostructure confines the electrons in the same region where the photon density is high, so that the interaction is strong. In other words, this structure focuses the light into the active region. The output of the laser is at about 9000Å.

In comparison the single heterostructure confines the light less effectively, and the homostructure (simple p–n junction laser) is even poorer. These structures also lack the preference for injecting electrons that the wide-gap emitter has; they rely primarily on the large ratio of electron mobility to hole mobility to achieve preferential injection of electrons.

For the single heterostructure the threshold increases again at small d. This increase may be caused by holes injected from the p-type active region backwards, into the emitter, when the electron population becomes large enough to reduce the injection of electrons.

The confinement of electrons to the active region reduces the temperature dependence of the threshold in these heterostructure lasers. The reduced temperature dependence is crucial for continuous lasing at room temperature.

For continuous operation we need a structure that maximizes heat dissipation. By combining the double hetero-

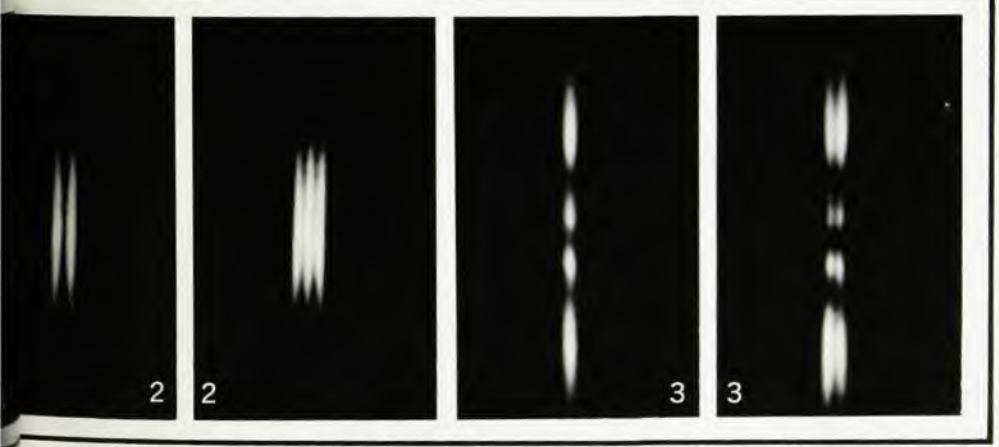

structure with stripe geometry, cw operation up to 355 K was achieved. Figure 7 shows such a structure, where a heat sink is bonded to the surface of the laser. The best available material for this purpose is type-IIa diamond, with a thermal conductivity of 20 W deg^{-1}cm^{-1}, four times more conductive than copper. At room temperature, these lasers have had a continuous power output of 40 mW.

If we want to obtain a certain wavelength in the range 7500Å–9000Å, we can include some aluminum in the active region. The concentration of aluminum outside the active region must be greater than the concentration inside to confine the electrons.

As in the homostructure lasers the stripe-geometry heterostructure laser has its output in a single filament, producing a well defined mode distribution. By controlling the thickness of the active region and the width of the stripe, we can excite modes of various orders, as seen in figure 1. These symmetrical modes are close to Hermite-Gaussian functions, and correspond to solutions of the wave equation in a dielectric waveguide with mirrors. The lowest-order, nearly Gaussian mode is produced when the active region is small enough (10-micron stripe width, 0.5-micron active region); here the power density at the mirror can be megawatts per cm^2. The peak power output is limited principally by destruction of the mirrors.

The most efficient junction lasers are grown from a solution of GaAs plus dopant (such as tin, zinc, silicon or germanium) in a solvent of aluminum and gallium. This procedure, known as liquid-phase epitaxy, has been refined to the point where layers less than a micron thick are grown.[7] The process requires multiple melts, corresponding to the layers indicated in the scanning electron micrograph (figure 8).

Second-order mode locking

Most lasers, solid state or gas, are particularly useful when operating with the phases of all optical modes synchronized ("locked") so that the total laser output (sum of all modes) is a series of narrow pulses with repetition rate ν_p equal to $\nu_{q+1} - \nu_q$, where ν_q and ν_{q+1} are consecutive longitudinal mode frequencies. The pulsewidth is approximately $1/\Delta\nu$, where $\Delta\nu$ is the width of the envelope of the locked-mode spectrum.

We can also view the mode-locked laser as a single-frequency source of frequency ν_q, amplitude modulated by a train of pulses of repetition rate ν_p. Fourier analysis shows that a series of sidebands with identical phase and frequency $\nu_q \pm n\nu_p$ (where n is any integer) are generated by the modulation; these sidebands are the other locked modes of the laser.

The semiconductor laser seems, at first glance, to be an ideal candidate for mode locking. Because separation between modes is inversely proportional to the size of the laser, its small size makes $\nu_{q+1} - \nu_q$ two orders of magnitude higher than for any other laser (about 10^{11}Hz). Its large gain linewidth allows many modes to operate, providing a large $\Delta\nu$ and correspondingly a very narrow pulse (about 10^{-13} sec). For photon energies near the forbidden band gap, however, where semiconductor lasers operate, the index of refraction is a strong function of the light frequency. This large dispersion leads to a nonconstant mode difference $\nu_{q+1} - \nu_q$ that has so far prevented conventional locking of any large number of modes. Although ways to compensate for this dispersion have been proposed,[14] they have not so far been realized.

The nonconstant mode difference combined with the nonlinearity of the lasing mechanisms does, however, allow locking of the modes through a higher-order interaction.[8] In this second-order mode locking, the total intensity is also a series of pulses. The repetition rate is, in the simplest case of second-order mode locking,

$$\nu_p = (\nu_q - \nu_{q-1}) - (\nu_{q+1} - \nu_q)$$

as is shown in figure 9.

Second-order mode locking, which has only been observed in semiconductor lasers, often occurs spontaneously when ν_p coincides with the frequency of the electron–photon interaction in the particular system, or it can be forced by external modulation.[8,9] Because of the high dispersion and small cavity size, the pulse repetition rate is of the order of 10^9 Hz. This value is higher than the rate achievable by conventional mode locking of most other lasers, and the pulse frequency is easier to stabilize and modulate than for other lasers. Pulsewidth is of the order of 100 picosec.

Emission delays

When we excite a junction laser with an externally applied pulsed current, there is a delay between the beginning of the current pulse and the onset of stimulated emission. Two distinct types

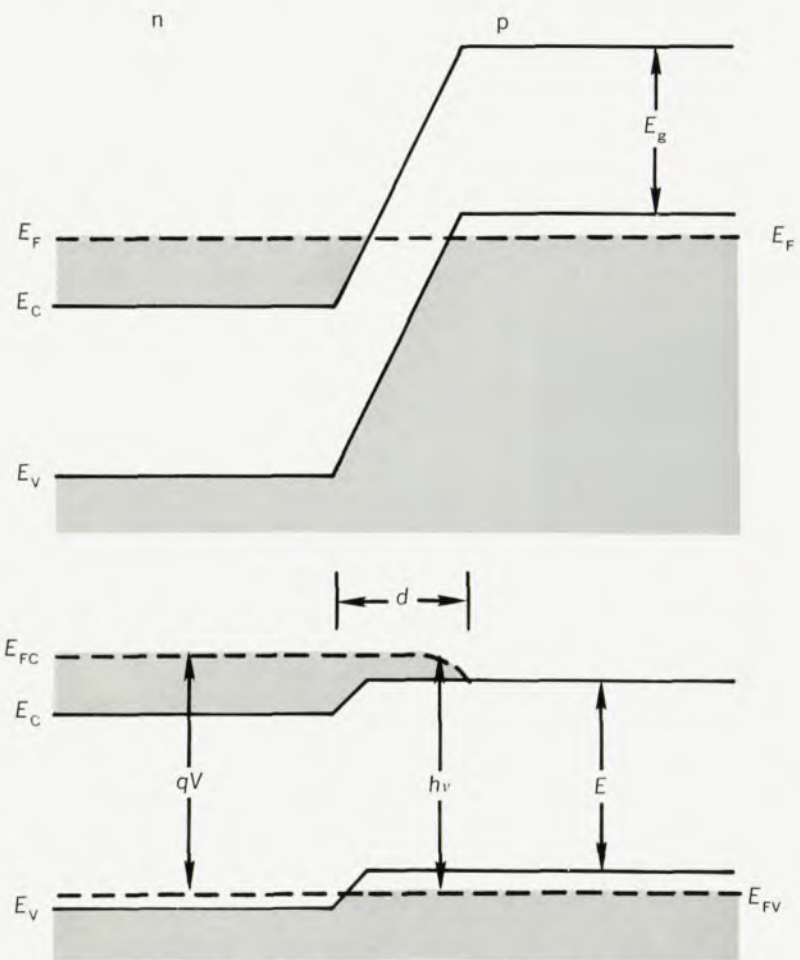

Energy-band diagrams of a p-n junction laser. Colored areas represent states filled with electrons. At zero bias (above) the Fermi level E_F is within both the valence and conduction bands, a situation known as "degenerate doping." Under a forward bias (bottom) large enough that qV, the product of the electron charge and the voltage across the junction, is larger than $h\nu$, (where ν is the frequency of the emitted light), the electron population is inverted. The region of population inversion d is the distance into the hole-rich p-region through which the electrons diffuse as they recombine with the holes. Figure 2

of delays have been observed. First, in all GaAs junction lasers at low temperatures, the delays are short (about 10^{-9} sec) and correspond to the time needed to produce the population inversion. Second, in many lasers the delays at room temperature are much longer (about 10^{-7} sec). The longer delays are consistent with the presence of saturable absorbing trapping centers.[10] As we vary temperature, we get an abrupt transition between short and long delays, and the value of the transition temperature depends on the fabrication procedure.

A double-acceptor trapping center can explain this behavior.[11] This trap can exist in three different states (see figure 10): doubly ionized, singly ionized or neutral (similar to a helium atom or ion in free space). At low temperatures all centers are doubly ionized and a first electron can be captured at an energy E_{12}. Because no states with the appropriate energy and crystal momentum exist in the valence band, the trap does not absorb photons of the lasing frequency in this state, and lasing is unaffected. As the temperature or injection current is increased, the trap captures electrons and is transferred to the singly ionized state Tr_2 where it can capture a second electron of energy E_{23}. E_{23} is higher than E_{12} because of the field of the first electron (the analogy with the helium ion is still valid). In this state the center can absorb the laser light by capturing an electron from the valence band. This absorption prevents lasing until a significant number of centers capture a second electron, transferring the centers to the third (neutral) state Tr_3. The neutral state will not absorb photons to excite electrons. In this way the trapping center produces the long delays.

A very interesting related effect will sometimes occur if a large number of centers remain absorbing at the end of the current pulse. When the current suddenly drops, some of these centers will lose their first electron and revert to the nonabsorbing, doubly ionized state Tr_1. If the absorption reduction is sufficient, a sharp Q-switched lasing pulse will occur *after* the end of the current pulse.[12] This effect is particularly dramatic in the single heterostructure where, because of the low thresholds, losses due to the trapping centers are a more significant portion of the total laser losses.

Saturable absorption by these traps can also produce bistability under cw conditions.[13] Once the laser turns on, it saturates many traps, reducing the losses so that it can stay on at a lower injection current.

Modulation

Ease of modulation is a characteristic of semiconductor lasers.[14] Amplitude,

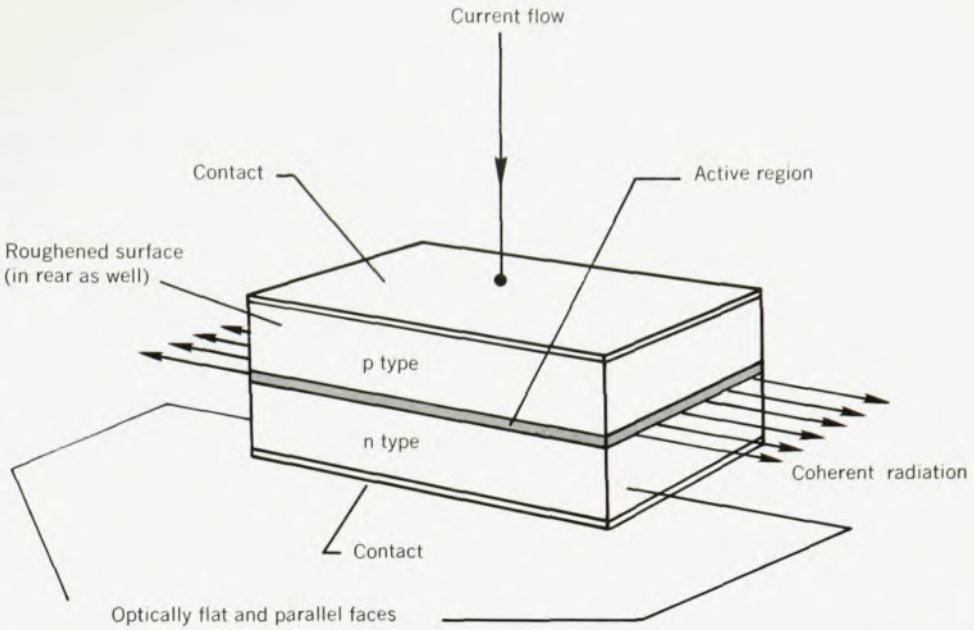

Simple p–n junction laser. Parallel crystal faces form the mirrors. Figure 3

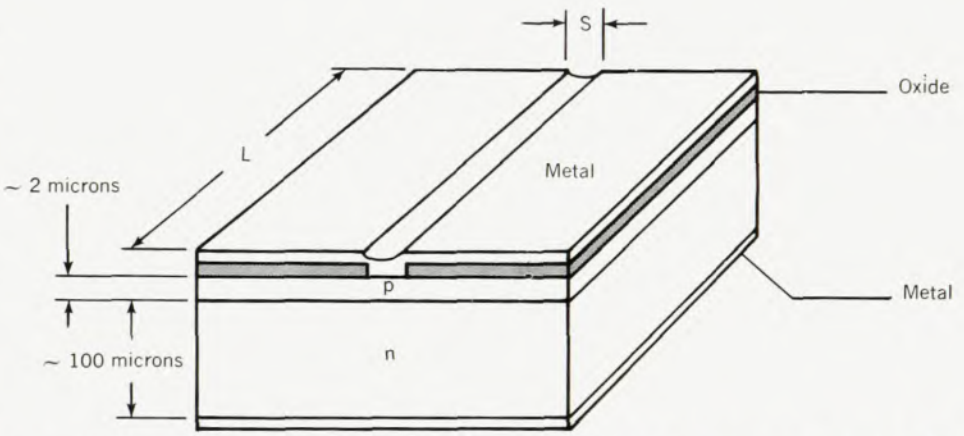

In a stripe-geometry laser, the active region is in the p-type layer directly below the stripe contact. Typical dimensions are (in microns): length 400, stripe width 12, active-layer thickness 2, total thickness 100. From ref. 26. Figure 4

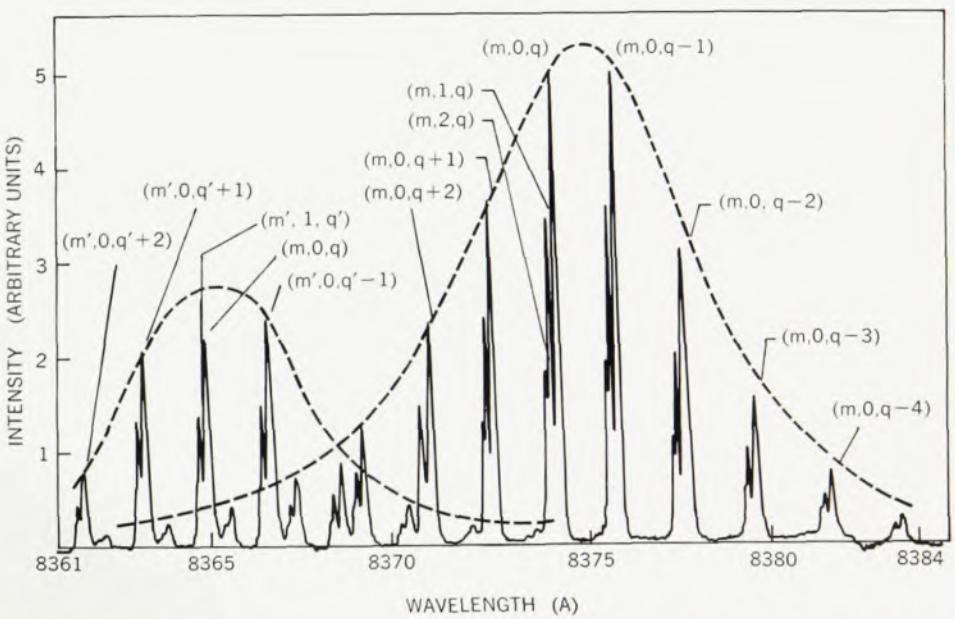

Spectrum of a continuously operating stripe-geometry GaAs laser. First integer (m) labels the modes perpendicular to junction; second labels transverse modes parallel to junction. Longitudinal modes (q) are 1.8 Å apart. From ref. 27. Figure 5

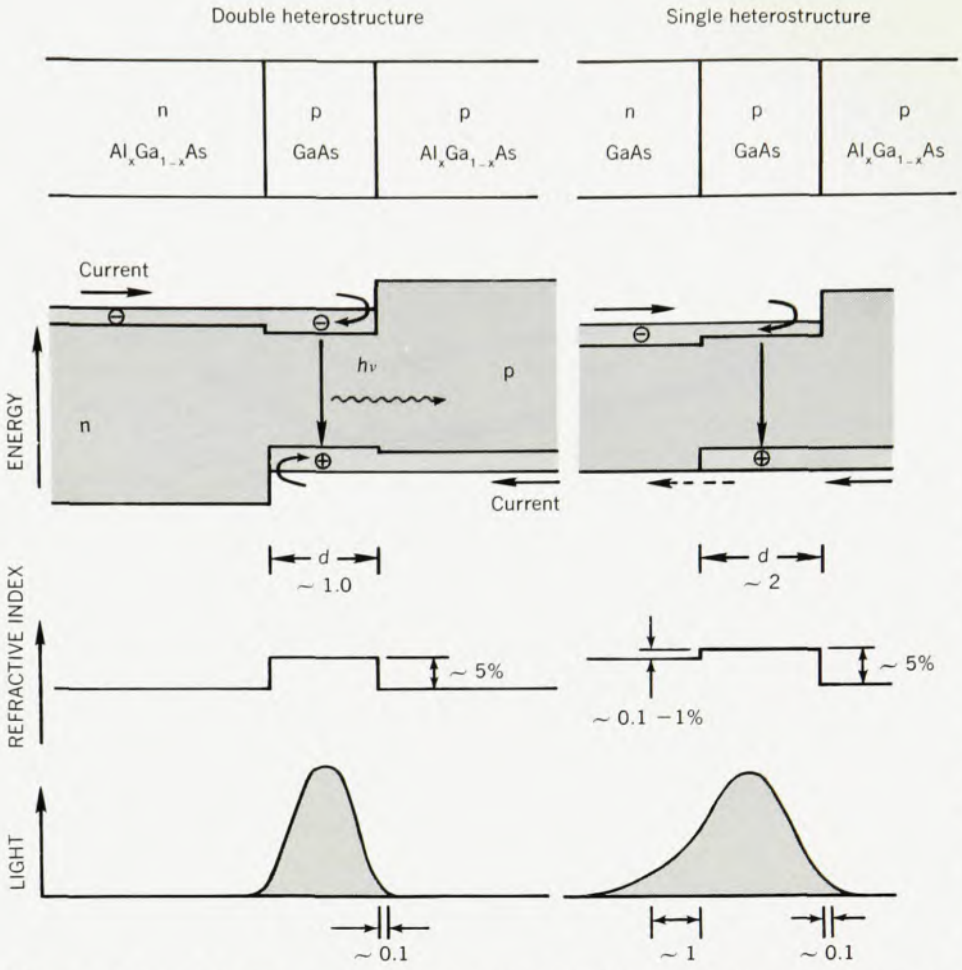

Characteristics of double and single heterostructure lasers. Schematic diagrams of energy bands under forward bias (top) show injection and recombination paths for electrons. The refractive indices of GaAs and $Al_xGa_{(1-x)}As$ differ by about 5% (center). Note (bottom) that the double heterostructure confines the light almost completely in the active region. Dimensions in microns. From ref. 28. Figure 6

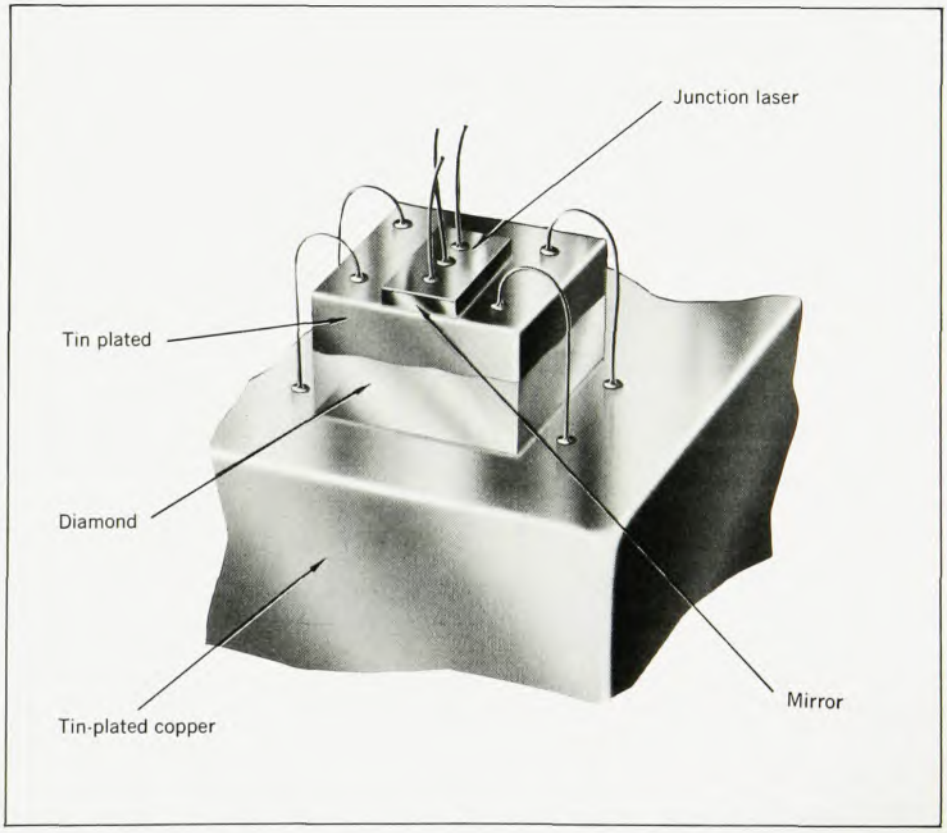

Laser on heat sink. Type-IIa diamond is preferred heat-sink material. Figure 7

frequency and pulse modulation are possible even at very high pulse rates.

The easiest way to modulate laser light is amplitude modulation, because the light intensity follows variations in the injection current. The short stimulated-emission lifetime (about 10^{-12} sec) and the short photon lifetime in the cavity (about 10^{-11} sec) permits modulation at microwave rates. Although modulation at 46 GHz has already been achieved, the modulation is linear only up to a few GHz because of a resonant interaction between the photon and electron population.

Varying the average index of refraction in the laser cavity varies the frequency of the laser modes. Two potentially fast methods that could accomplish this frequency modulation have been proposed. In the first method[15] the laser cavity is divided into two regions, one of which is kept below threshold and is then modulated. Substantial dielectric-constant changes occur in this region, and these changes result in changes of the mode frequencies of the overall cavity. The second method uses the pressure dependence of the dielectric constant. When ultrasonic waves are sent in a direction perpendicular to the cavity the dielectric constant varies with the instantaneous sound pressure, modulating the laser frequency. Modulations up to 5×10^8 Hz have been achieved and the theoretical limit is an order of magnitude higher.

The pressure-dependence method is the only method not affected by the photon–electron interaction resonance, because sound waves affect both electron and photon populations only slightly. For the same reason, we get frequency modulation with negligible amplitude modulation or mode distortion.

The simplest kind of pulse modulation uses the laser to get an optical replica of the previously modulated electrical signal. The delays between application of the injection pulse and the start of stimulated emission are minimized by prepumping the laser up to just below threshold instead of starting from zero bias.

A potentially faster method uses the second-order mode locking we have discussed. Because resulting pulses can be locked to an external microwave signal with power of only a fraction of a milliwatt, frequency modulation of this signal results in pulse-position modulation of the laser pulses. This modulation can be achieved up to a rate equal to half the spontaneous pulsing frequency, that is in a range from 0.3 to 3×10^9 Hz.

IV–VI lasers

The lead chalcogenides (compounds between lead and elements in group VI of the periodic table) and their com-

pounds form a group of junction lasers whose physics is very interesting: Because of the small forbidden gaps in these compounds, recombination takes place band-to-band instead of involving impurity bands as in GaAs, providing a way to study the band structures; the forbidden-energy gap, and consequently the laser frequency, can be tailored over a wide range by varying pressure or temperature, or alloying with tin chalcogenides; the four equivalent band gaps at the 111 edges of the Brillouin zone can be split away from their degeneracy by uniaxial pressure or magnetic field.

A group at Lincoln Laboratory, MIT, has done most of the work on these junction lasers, including the first successful operation with lead telluride, lead selenide and lead sulfide.

Because the forbidden-energy gap of the lead-salt lasers contracts with pressure (in contrast with the III–V GaAs semiconductors), a large range of tuning of these lasers is possible by varying either uniaxial or hydrostatic pressure.[16] This tuning was accomplished, using liquid helium as the pressure-transmitting fluid and PbSe lasers were tuned from 8 microns to 22 microns.[17] These were the first lasers tunable over such a wide range.

Uniaxial pressure in a direction other than 100 can also split the degeneracy of the conduction and valence bands, eventually turning the material into an indirect-gap semiconductor. This transformation was done with an optically pumped 110 strained, p-type PbSe crystal.[18] As the fourfold band degeneracy splits into two twofold-degenerate bands with energy gaps E_{g1} and E_{g2} (figure 11), two types of behavior are observed. When ΔE_c, the energy difference between the conduction bands, is smaller than the 002 phonon energy E_p connecting the two sets of edges, no interband transitions are possible, because the low temperature prevents phonon absorption. Under these circumstances, both E_{g1} and E_{g2} lines lase. As the pressure increases, and ΔE_c reaches E_p the 111 and $11\bar{1}$ conduction-band edges are rapidly emptied by phonon emission, and we see only the E_{g2} lasing line. The large emission of phonons with identical momentum raises the possibility that a phonon laser can be produced simultaneously with the E_{g2} laser, although there is no experimental proof of this idea.[18] As the pressure increases further, all holes are transferred to the 111 and $11\bar{1}$ valence-band edges, and the transition from direct to indirect semiconductor is complete. Lasing is now impossible.

By making diodes from lead–tin chalcogenide alloys, we can tailor the laser frequency, and varying current and temperature provides further tuning. These alloys lase at wavelengths as long as 28 microns,[19] the longest wavelengths obtained in any junction laser to date. Lasers that operate near 10.6 microns can be heterodyned with carbon-dioxide lasers,[20] allowing determination of the shape of the laser diode line (Lorentzian, and as narrow as 54 kHz) and its spatial distribution (second-order Hermite-Gaussian for one sample).[21] The narrowness of the line and its tunability by current variations make it useful in very high resolution spectroscopy in the far-infrared.

The laser frequency depends on salt composition, supporting the hypothesis[22] that $Pb_{1-x}Sn_xTe$ and $Pb_{1-x}Sn_xSe$ have conduction and valence bands of different symmetries[23] for small and large x. The temperature dependence of the laser frequency,[24] with $d\nu/dT$ negative for small x and positive after

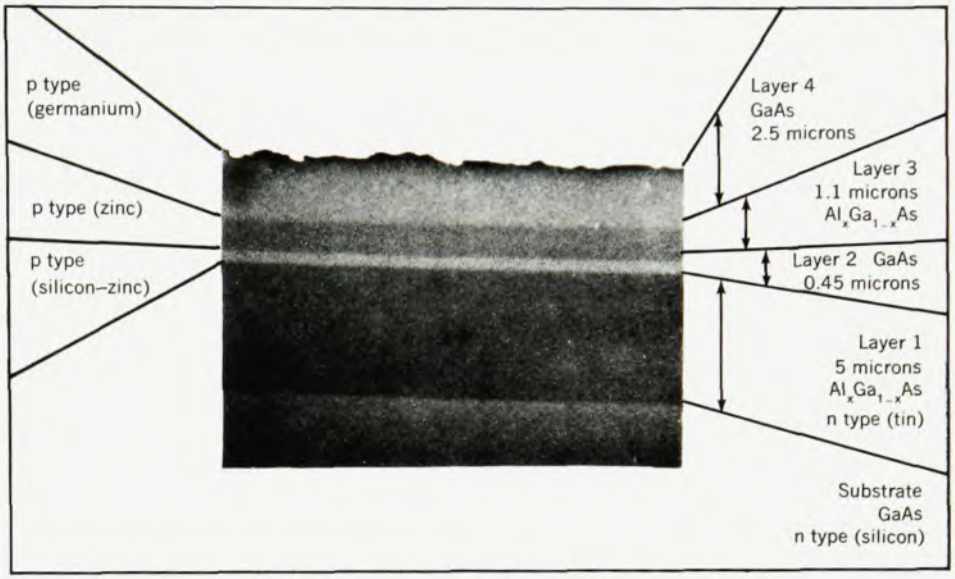

Scanning electron micrograph shows the cleaved face of a junction laser that was grown by the liquid-phase epitaxy method. From ref. 7. Figure 8

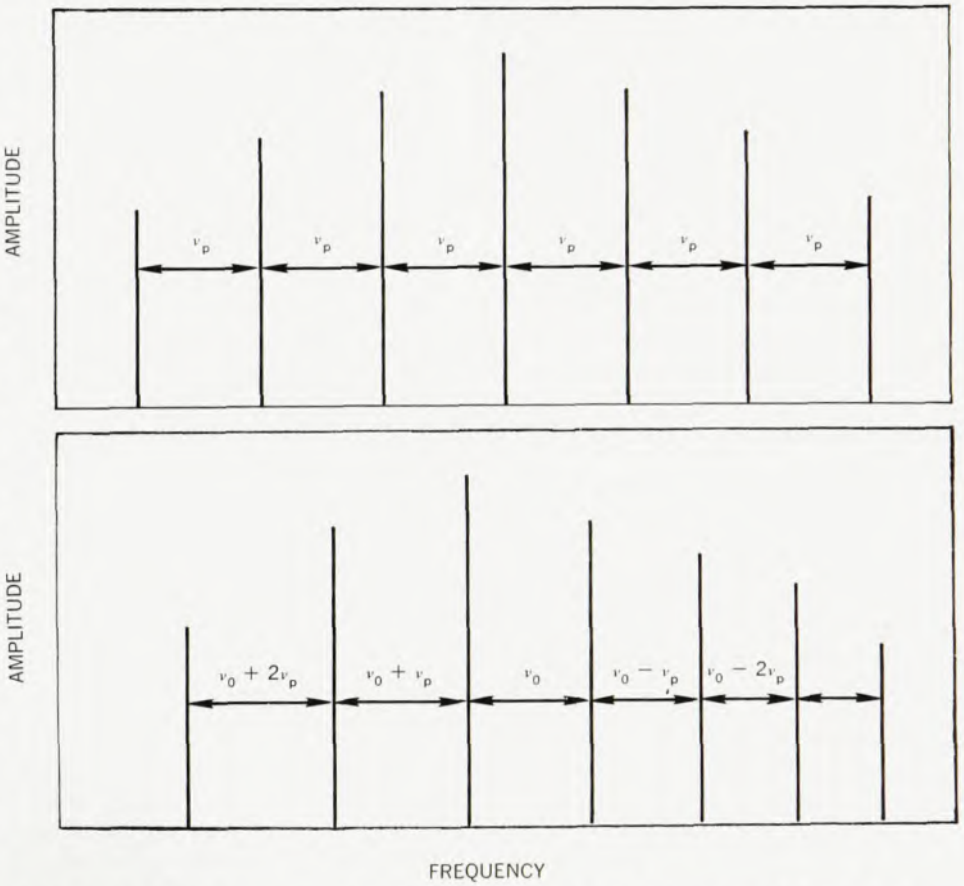

Mode spacings for conventional mode locking (top) and second-order mode locking.. Pulse repetition rate in second-order case is of the order of 10^9 Hz. Figure 9

the crossover, confirms the result, as does the magnetic-field dependence[25] of the laser frequency for the various compositions. These later experiments also measure the effective masses and g-factors of the laser materials.[25]

Work on junction lasers and semiconductor lasers has resulted in a large body of new knowledge of semiconductor physics. Band structure properties in III–V and IV–VI compounds, energy levels, impurity bands, recombination processes and properties of heterostructures with low recombination velocity are a few of the topics where advances have been made.

Future junction lasers will probably have higher power outputs, with improved mode control and will operate at visible wavelengths. Because of their small size, high efficiency, mechanical ruggedness and especially their low cost, junction lasers may ultimately become the most widely used of all lasers.

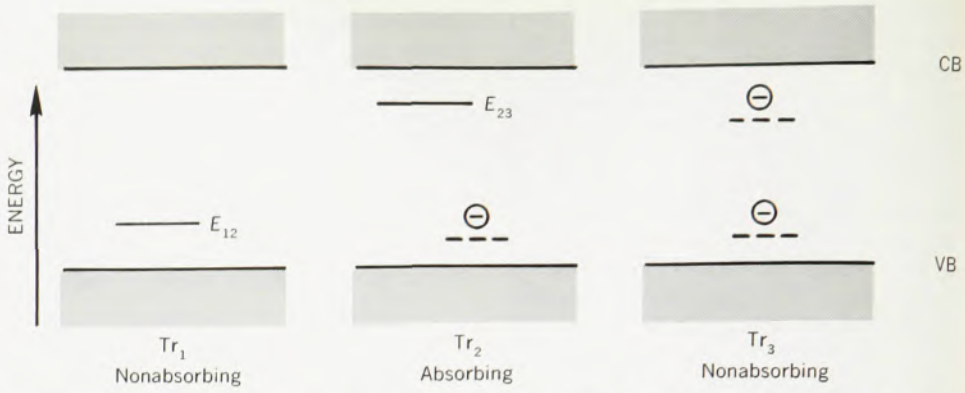

Acceptor trap model for time delays and Q-switching in GaAs junction lasers. The trap can exist in three states. One electron can be captured at energy E_{12} and a second electron at energy E_{23}. From ref. 30. Figure 10

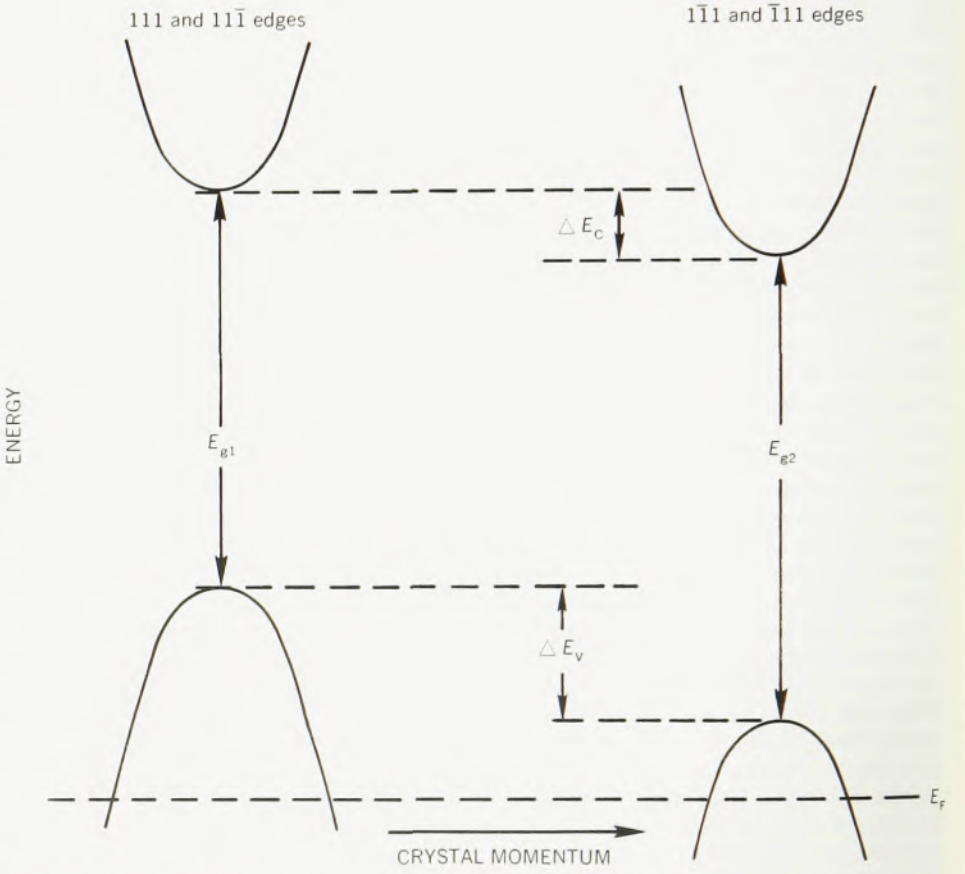

In p-type lead selenide, a stress in the 110 direction splits the fourfold degeneracy of the conduction and valence bands into twofold-degenerate bands with energy gaps E_{g1} and E_{g2}. Increasing the pressure changes the lead selenide to an indirect-gap semiconductor. From ref. 18. Figure 11

References

1. G. Burns, M. I. Nathan, Proc. IEEE, **52,** 770 (1964); M. I. Nathan, Proc. IEEE, **54,** 1276 (1966); C. H. Gooch, *Gallium Arsenide Lasers,* Interscience, London (1969); S. M. Sze, *Physics of Semiconductor Devices,* Interscience, New York (1969), page 687.
2. I. Hayashi, M. B. Panish, P. W. Foy, S. Sumski, Appl. Phys. Lett. **17,** 109 (1970).
3. M. G. A. Bernard, G. Duraffourg, Physica Status Solid **1,** 699 (1961).
4. A. K. Jonscher, M. H. Boyle, *Gallium Arsenide: 1966 Symposium Proceedings,* IPPS, London (1967).
5. D. K. Wilson, in *Radiative Recombination in Semiconductors,* Academic, New York (1964), page 171.
6. W. E. Ahearn, J. W. Crowe, IEEE J. Quantum Electronics **QE-2,** 597 (1966).
7. M. B. Panish, S. Sumski, I. Hayashi, Metallurgical Trans. (to be published).
8. T. L. Paoli, J. E. Ripper, Phys. Rev. Lett. **22,** 1085 (1969).
9. T. L. Paoli, J. E. Ripper, Appl. Phys. Lett. **15,** 105 (1969).
10. G. E. Fenner, Solid-State Electronics **10,** 753 (1967).
11. J. E. Ripper, IEEE J. Quantum Electronics, **QE-5,** 391 (1969).
12. J. E. Ripper, J. C. Dyment, Appl. Phys. Lett. **12,** 365 (1968).
13. J. E. Ripper, T. L. Paoli, J. C. Dyment, IEEE J. Quantum Electronics **QE-6,** 300 (1970).
14. T. L. Paoli, J. E. Ripper, Proc. IEEE **58,** 1457 (1970).
15. G. E. Fenner, Appl. Phys. Lett. **5,** 198 (1964).
16. G. W. Pratt, J. E. Ripper, J. Appl. Phys. **36,** 1525 (1965).
17. J. M. Besson, J. F. Butler, A. R. Calawa, W. Paul, R. H. Rediker, Appl. Phys. Lett. **7,** 206 (1965).
18. G. W. Pratt Jr, P. G. McMullin, in *Proceedings* of the Tenth International Conf. on the Physics of Semiconductors, Cambridge, Mass. (1970).
19. J. F. Butler, T. C. Harman, Appl. Phys. Lett. **12,** 347 (1968).
20. E. D. Hinkley, T. C. Harman, C. Freed, Appl. Phys. Lett. **13,** 49 (1968).
21. E. D. Hinkley, C. Freed, Phys. Rev. Lett. **23,** 277 (1969).
22. J. O. Dimmock, I. Melngailis, A. J. Strauss, Phys. Rev. Lett. **16,** 1193 (1966).
23. J. B. Conklin Jr, L. E. Johnson, G. W. Pratt Jr, Phys. Rev. **137A,** 1282 (1965).
24. T. C. Harman, A. R. Calawa, I. Melngailis, J. O. Dimmock, Appl. Phys. Lett. **14,** 333 (1969).
25. J. F. Butler, Solid State Commun. **7,** 909 (1969).
26. J. C. Dyment, Appl. Phys. Lett. **10,** 84 (1967).
27. T. L. Paoli, J. E. Ripper, T. H. Zachos, IEEE J. Quantum Electronics **QE-5,** 271 (1969).
28. I. Hayashi, M. B. Panish, F. K. Reinhart, J. Appl. Phys. (to be published).
29. J. E. Ripper, J. C. Dyment, L. A. D'Asaro, T. L. Paoli, Appl. Phys. Lett. **18,** 155 (1971).
30. J. C. Dyment, J. E. Ripper, IEEE J. Quantum Electronics **QE-4,** 155 (1968).

□